RESEARCH PAPER

Optical and Gas Sensing Properties of Pr-Doped TiO_2 Thin Film

Baskaran Revathi, Perumal Perumal*, Deivanayagam Deivamani

* *perumal59@gmail.com*

PG and Research Department of Physics, Alagappa Government Arts College, (Affiliated to Alagappa University, Karaikudi) Karaikudi-630 003, India

Received: July 2022 **Revised: May 2023** **Accepted: May 2023**
DOI: 10.22068/ijmse.2892

Abstract: *In this research, praseodymium (Pr) doped titanium oxide was deposited onto a glass substrate by nebulizer spray pyrolysis technique. The rare-earth-doped thin film was subjected to studies on structural, morphological, optical, and gas-sensing properties. The structural properties of the deposited thin films exhibit varied texture along with (101) direction. The grain size of the thin film varies with various mole percentages of doped TiO_2 thin films. As various doping concentrations increase, the prepared thin films show different optical properties like band gap, extension coefficient, refractive index, and dielectric constant. Fourier transform infrared (FTIR) results revealed that the reflectance spectra conformed to the existence of functional groups and chemical bonding. Gas sensing studies were carried out for undoped and Pr-doped TiO_2 films. The sensor was exposed to ethanol gas. The response of a TiO_2 thin film at different ethanol concentrations and different operation temperatures was studied. The gas sensitivity of ethanol gas was measured when the fast response of the film with 0.004M Pr-doped TiO_2 thin film showed a response time of 99 s and recovery time of 41 s, as well as the resistance falling to $0.6X10^6$ Ω. The sensor operated at maximum effectiveness at an optimum temperature of 200°C.*

Keywords: *Doped TiO_2 thin films, Structural properties, Optical properties, Gas sensor studies.*

1. INTRODUCTION

Titanium dioxide (TiO_2) thin films have been studied due to their attractive general properties for photocatalysis, sensor, and anti-bacterial agent. TiO_2 thin film has a wide range of applications due to its electronic and structural properties. The potential applications of TiO_2 thin film use solar cells [1], optoelectronic devices [2], as well as being extensively used for the detection of gas sensors, etc. [3–4]. Sensors can be made of different materials, depending on their purposes, so it is necessary to evaluate the physical and chemical properties of the compounds involved in the formation of gas sensors to attain the best results in detecting various gases [5]. In recent years, researchers have suggested that TiO_2 thin film with doping of rare earth elements would enhance and can be used for different applications. Recently, metal oxides have been very useful for detecting various gases. Un-doped and doped TiO_2 films have been investigated as sensors for many different gases, such as propanol, methanol, and ethanol [6], H_2 [7], NO_2 [8], CO [9], and NH_3 [10]. One of the necessities of gas sensors is their low power consumption and their need to work reliably and continuously. TiO_2 is a metal oxide semiconductor, which is widely used for gas sensor applications due to its electrical properties. Nowadays, there are numerous thin film synthesis methods; spray pyrolysis is one of these methods [11–14]. Besides, various routes have been used for spray methods, such as chemical vapor deposition, atomic layer deposition, the RF magnetron sputtering method, and pulsed laser deposition [15–17]. However, nebulizer spray pyrolysis is one of the most widely applied methods because it is easy, cheap, and handy. This preparation method is cost-effectively feasible and can be applied to substrates with large surfaces and different forms. In the present study, un-doped TiO_2 and Pr-doped TiO_2 thin films deposited by nebulizer spray pyrolysis were subjected to structural, optical, morphological, and sensor characterization. Our results demonstrate an excellent promise for change in the optical and structural behavior of the TiO_2 thin films, with a potential approach toward sensor devices.

2. EXPERIMENTAL PROCEDURES

Titanium dioxide thin films were synthesized using the Nebulizer Spray Pyrolysis Method. For the preparation of TiO_2 thin films, high-purity chemicals (>99% purity), such as titanium tetra chloride ($TiCl_4$) (Sigma–Aldrich), were used as precursors without further purification. For doped

[DOI: 10.22068/ijmse.2892]

material, high-purity chemicals (>99% purity; Sigma-Aldrich) such as praseodymium oxide (Pr_2O_3) were used. FTO-coated glass measuring 20x20 mm in size has been used as a substrate to deposit TiO_2 thin films. Substrate cleaning plays a major role in thin film deposition. Hence, the substrate is cleaned by an ultrasonicator with distilled water, ethanol, and propanol solutions of the same ratio for 10 minutes and then left to dry in the air. In this work, the TiO_2 thin films were deposited at constant precursor concentrations of 0.1 M and dissolved in deionized water. The parameter of this experiment is the substrate temperature, which was constrained by an iron-constantan type thermocouple and kept constant at its optimized value of 350°C. The spray rate of the precursor solution and the period for each spraying were fixed at 1.0 mL/s. The praseodymium (Pr) solutions of 0.004M and 0.008M were mixed with a titanium precursor solution to prepare Pr-doped TiO_2 thin films. The schematic diagram of an experimental set-up for the Nebulizer Spray Pyrolysis Technique is shown in Fig. 1. The precursor solution was held in the nebulizer unit, which is linked to an air compressor. The mist-like, tiny droplets of particles were carried from the glass tube to deposit on the glass substrate kept in the homogeneous hot zone of the furnace. After deposition, the films were permitted to cool at room temperature and then preserved in desiccators. The quality of thin films was studied by their structural properties using X-ray diffraction (XRD), morphology using field emission scanning electron microscopy (FESEM), and optical properties using UV-Vis spectroscopy. The FTIR spectra of the thin films were recorded using a Fourier transmission infrared spectrometer ("Thermo Nicolet 380") in the range of 400–4,000 cm^{-1}. The deposited pure and Pr-doped TiO_2 films were used for gas-sensing properties. The gas response study of the film was measured before and after exposure to ethanol vapor using a Keithley 2400 source meter. The film's sensing characteristics at different ethanol concentrations were studied at different operating temperatures. Resistance measurement and gas response sampling are carried out at an optimum temperature of 200°C. The sensitivity of the experiment was defined as the ratio of air resistance to gas resistance.

3. RESULTS AND DISCUSSION

3.1. X-ray Diffraction Analysis

Praseodymium doped and undoped TiO_2 thin films were characterized by the X-ray diffraction technique (Fig. 2) to analyze the effect of praseodymium at various concentrations.

X-ray diffraction patterns were recorded to identify the deposited film-formed polycrystalline phases. The diffraction peaks indicate that the thin films possess a polycrystalline nature with an anatase phase. It is observed from Fig. 2(a), which revealed that the undoped TiO_2 deposited films exhibit a tetragonal body-centered cubic structure [ICDD File No.: 89-4203].

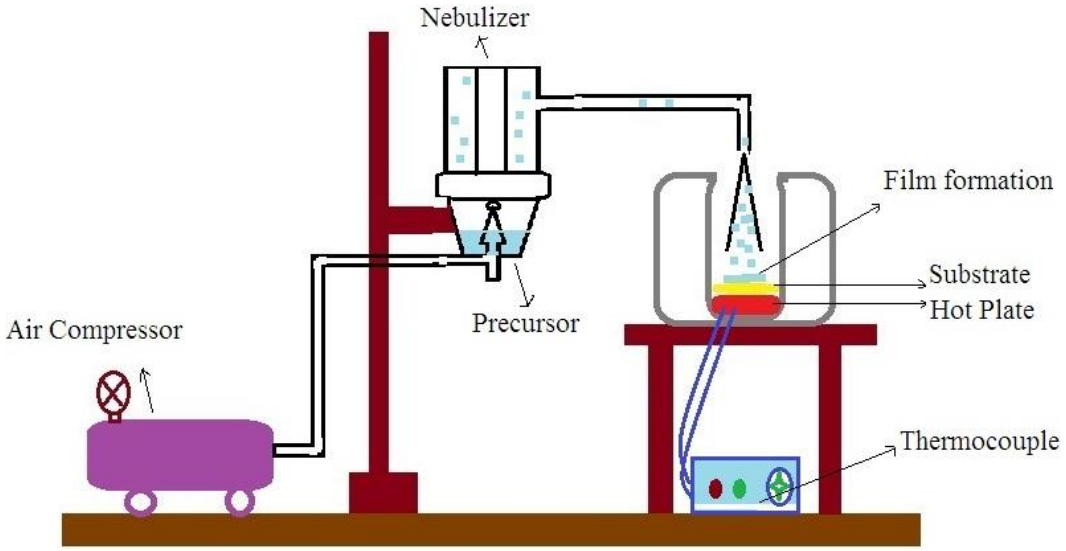

Fig. 1. Nebulizer spray pyrolysis experimental setup

[DOI: 10.22068/ijmse.2892]

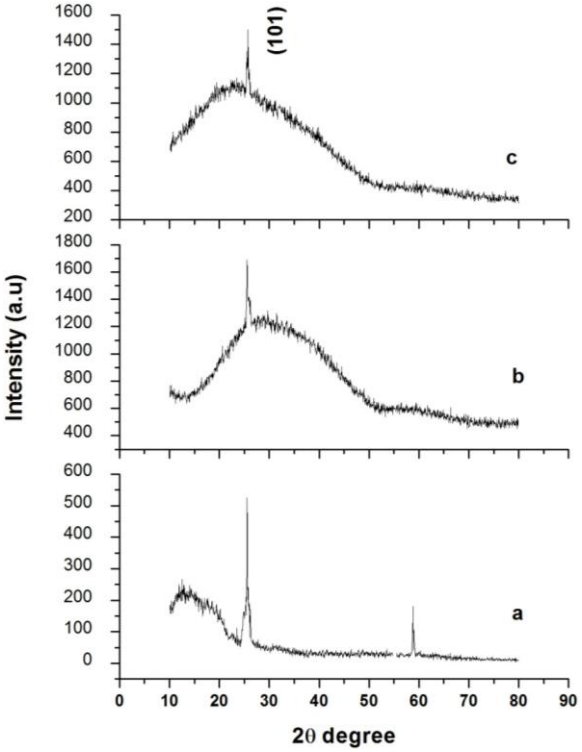

Fig. 2. X-Ray Spectrograph: a) Undoped TiO_2 Thin Film; b) 0.004 M Pr Doped TiO_2 Thin Film; c) 0.008 M Pr Doped TiO_2 Thin Film.

The observed diffraction peaks of the tetragonal TiO2 are found at a 2θ value of 25.35° and 55.05°, respectively, which correspond to the lattice planes (101) and (211). The observed peak of the undoped TiO_2 is present in the pattern of the anatase phase. Fig. 2(b) shows the X-ray diffraction pattern of 0.004M Pr- doped TiO_2; according to the way, the anatase crystal structure has not been influenced by Pr- doping. The doped TiO_2 has only one (101) plane compared with the undoped XRD pattern. The approach of doping materials in the TiO_2 film has a lattice that induces slight expansion, leading to the doped material's large ions. Fig. 2(c) shows the peak intensity decreased by a 0.008 M Pr-doped TiO_2 thin film. From the full width and a half maximum of the preferential orientation peak (101), the crystalline grain size is calculated in Table 1. The crystalline size D was calculated from the preferential (101) diffraction peaks using Debye-Scherrer's equation (1) [18];

$$D= 0.9\lambda/(\beta \cos\theta) \quad (1)$$

Where 'λ' is the wavelength of the X-ray used (λ= 0.1540 nm), 'β' is a full-width half maximum of the peaks in radians, and 'θ' is the Bragg's diffraction angle at the peaks position in degrees. The variation of crystalline size concerning pure and Pr-doped TiO_2 is shown in Table 1. As the doping atom exerts a drag force on boundary motion and grain development, crystalline size decreases with increasing Pr doping concentration. And dislocation density was calculated using relation [18],

$$\delta=1/D^2 \quad (2)$$

The lower value δ from Table 1 for low Pr doped TiO_2 thin film has few lattice defects and good crystalline qualities.

3.2. Optical Properties

The UV–visible spectrum analysis of the undoped and Pr-doped TiO_2 thin film was shown in Fig. 3. In the visible region of the solar spectrum, the transmission is approximately 95% undoped TiO_2, 89% low Pr-doping, and 93% high doping. Praseodymium has three oxidation states; most of it forms the +3 oxidation state, which is the only stable state in an aqueous solution. Although the +4 oxidation state is known in a few solid compounds and exclusively among the lanthanides, the +5 oxidation state is attainable in a matrix-isolation situation. The visible transmission of these films increases with increased Pr concentration due to the improved oxidation of the film. The optical transmittance spectra of the pure and Pr-doped thin films in the wavelength range of 300 to 800 nm were shown in Figure 3. The figure shows a significant visible region shift with increasing doping levels. When doping increased in the thin film, it became highly transparent in the visible range. The optical transmittance of the pure and Pr-doped films is above 70% in the visible region. As doping concentration increases, Pr-doped TiO_2 films show that the transmittance increases up to above 90%.

Table 1. The variation of crystalline size concerning pure and Pr-doped TiO_2

Thin films	Thickness(nm)	Phase	Crystalline size (nm)	Dislocation Density×10^{14}lines/m^2
UndopedTiO_2	200	Anatase	43	5.408
0.004 M Pr Doped	260	Anatase	57	3.027
0.008 MPr Doped	295	Anatase	51	3.749

[DOI: 10.22068/ijmse.2892]

This increase in transmittance is attributed to the fine crystallization in the deposited films.

We have recorded the optical transition spectra values of Pr-doped and undoped TiO_2 at room temperature, and the transition spectra were used to calculate the refractive index using the envelope method proposed by Swanepoel [19].

$$n= [N_1+(N_1^2+S^2)^{½}]^{½} \quad (3)$$

$$N_1 = 2S\frac{T_M-T_m}{T_M T_m}\frac{(s^2-1)}{2} \quad (4)$$

T_M and T_m are the value of the maximum and minimum transition values at particular wavelengths. 'S' is the refractive index of the substrate. The optical constants were estimated in the wavelength range of 300 to 800 nm, and a fabulous interference pattern was observed in the transmission spectra range.

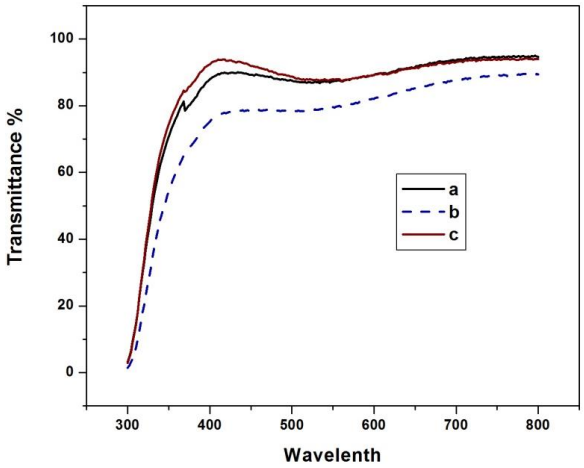

Fig. 3. Optical transmittance of a) undoped TiO_2 b) 0.004 M pr-doped TiO_2 c) 0.008 M pr- doped TiO_2

The refractive index of the Pr-doped and undoped TiO_2 thin films was calculated using envelope methods, and the values are plotted as a function of wavelengths as shown in Fig. 4. When low doping concentration TiO_2 is used, the refractive index value is high, and when high-doping concentration TiO_2 thin film is used, the value decreases. The value of the refractive index lies between 1.6 and 1.9 for pure TiO_2 and Pr-doped TiO_2 thin films. This change can be attributed to higher packing density and a change in the crystalline structure, with the latter increasing as well as crystallization growth [20]. The reduction of the 'n' value with doping incorporation and end reaches a just about constant level [21].

The variation of the extinction coefficient (K) with wavelength for TiO_2 thin film is shown in Fig. 5. The prepared TiO_2 thin films' extinction coefficient (K) was calculated using the equation [22] $K= \alpha\lambda/4\pi$, where λ is the wavelength of the incident photon energy. Figure 5, depicts the extinction coefficient deviation with wavelength for pure and Pr-doped thin TiO_2 films. The value of the extension coefficient of Pr-doped TiO_2 increases at a low concentration of Pr doping, depending on the band gap of anatase TiO_2. The decreasing behavior of high doping depends on light absorption at grain boundaries [23].

The extinction coefficient of prepared pure TiO_2 and Pr-doped thin films has a value range of 0.07–0.11, and the low value of Pr doping leads to the homogeneity of the deposited film. The optical properties of the band gap (Eg) of TiO_2 doped and undoped films can be calculated in the following relation [24–25].

$$(\alpha h\upsilon)^2= C(h\upsilon-Eg) \quad (5)$$

Where $h\upsilon$ is photon energy, C is constant, and α is the absorption coefficient, which can be calculated by equation [26].

$$A= 1/d \ln 1-R/T \quad (6)$$

Where 'd' is the film thickness, The plot $(\alpha h\upsilon)^2$vs $h\upsilon$ (Fig.(6)) determines the range of 3.57 to 3.75 eV. The band gap is plotted [25] as a function of Pr doping concentrations, as shown in Fig. 5. It is observed that the band gap of undoped TiO_2 is 3.67 eV, and the band gap decreases to 3.57 eV at a low doping concentration. The widening of the optical band gap is 3.75 eV which is related to increases in higher Pr doping concentration. The optical properties of the thin film were highly affected by the crystallite size of the materials [27].

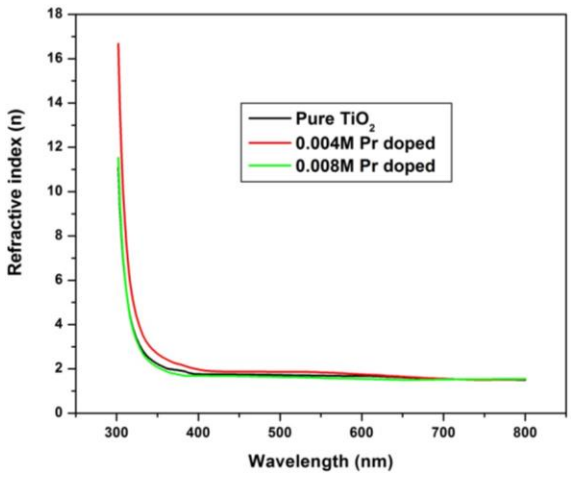

Fig. 4. Variation of refractive index (n) versus wavelength for pure and Pr-doped TiO2 thin films

[DOI: 10.22068/ijmse.2892]

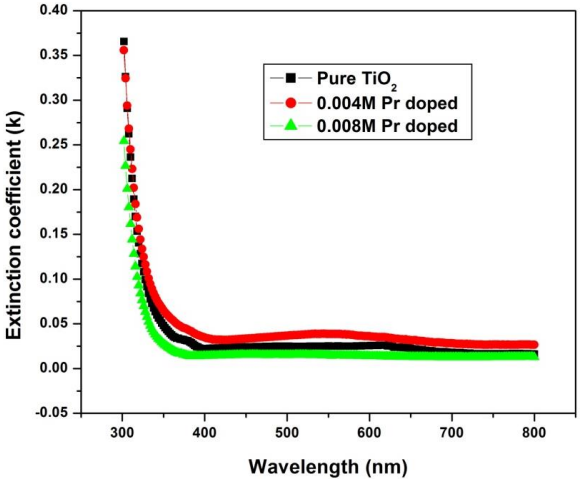

Fig. 5. Variation of extinction coefficient (k) versus wavelength for pure and pr-doped TiO_2 thin films

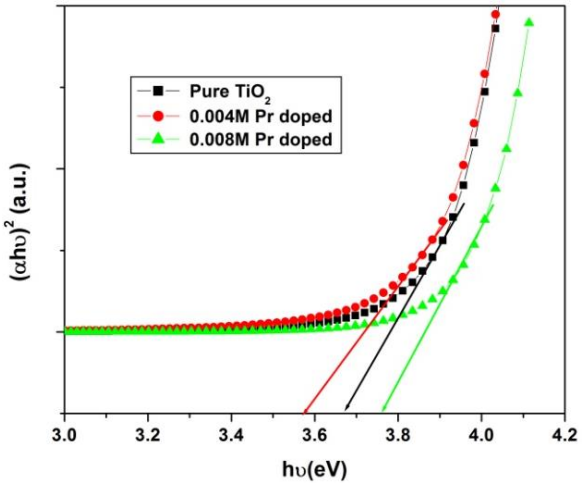

Fig. 6. Tauc's plot of TiO_2 thin film prepared at pure and pr-doped thin films

3.3. Surface Morphology

The surface morphology of pure and Pr-doped TiO_2a thin film was investigated using field emission scanning electron microscopy (FE-SEM). Figure.7 shows the SEM images of pure and Pr-doped TiO_2 thin films. A pure TiO_2 film shows the Powderly coated grain clusters (Fig. 7a). Further, pure TiO_2 owns the unevenly distributed fine grains with sizes of ~50 nm. A similar observation was made for TiO_2 thin films earlier.

FESEM explores porous, structured grains of smaller sizes for a low amount of Pr-doped TiO_2 thin films. The doped thin film's grain sizes are considerably reduced compared to those of pure TiO_2 thin films, leading to enhanced sensitivity properties (Fig. 7b). And a high amount of Pr-doped thin films (Fig. 7c) have a porous structure with agglomerated clustered nanocrystalline grains.

3.4. FTIR Spectra Analysis

The FTIR spectra of the Pr-doped TiO_2 thin films are shown in figure 8. The FTIR films were taken in the range of 300–4000 cm^{-1}. The stretching and bending vibrations of O-H hydroxyl groups show bands at 3,400 and 1,620 cm^{-1}. From Figure 8, the spectra show absorption peaks in the range of 3400-3500 cm^{-1}. The –OH stretching vibration of the hydroxyl group is absorbed on the different active sites of the TiO_2 material. The maximum strength of the peak is shown in a high-doped TiO_2 thin film. The Ti-O-Ti of oxygen vibration has a frequency presence in the 400-500 cm^{-1} region**.**

3.5. Gas sensitivity measurement

The variation of resistance and gas sensitivity of pure TiO_2 and Pr-doped TiO_2 thin films are shown in Fig. 9. Generally when a specific gas molecule is absorbed, the electrical properties of the metal oxide will change. When the material is exposed to an ethanol environment, metal oxide sensing properties can be detected as a change in electrical resistance. When ethanol molecules interact with absorbed oxygen ions on the surface of TiO_2 nanostructures, they can release free electrons back into the conduction band, which leads to an increase in the conductivity of the TiO_2 structure [28].

Figure 9(A) illustrates the pure TiO_2 thin film response and recovery time graph with a 200 ppm ethanol concentration at 200°C. It shows that resistance gradually decreases from 2.5×10^6 Ω (air) to 1.5×10^6 Ω (gas), with response times of 156 s and recovery times of 62 s, respectively. The observed response and recovery time of different doping concentrations with pure TiO_2 thin film are shown in Fig. 9 (B–C). Figure 9(B) offers a 0.004 M Pr doped TiO_2 thin film with a response time of 99s and a recovery time of 41 s; the resistance of 0.6×10^6 Ω falls more than that of pure TiO_2. The effectiveness of grain-linked formation by pr-doping controlled by inter-grain potential contributes to gas sensing properties [29]. Compared with pure TiO_2, both response and resistance were decreased due to oxygen ions reacting on the surface and the increased number of free electrons that led to better conduction in the Pr-doped TiO_2 nanostructure.

[DOI: 10.22068/ijmse.2892]

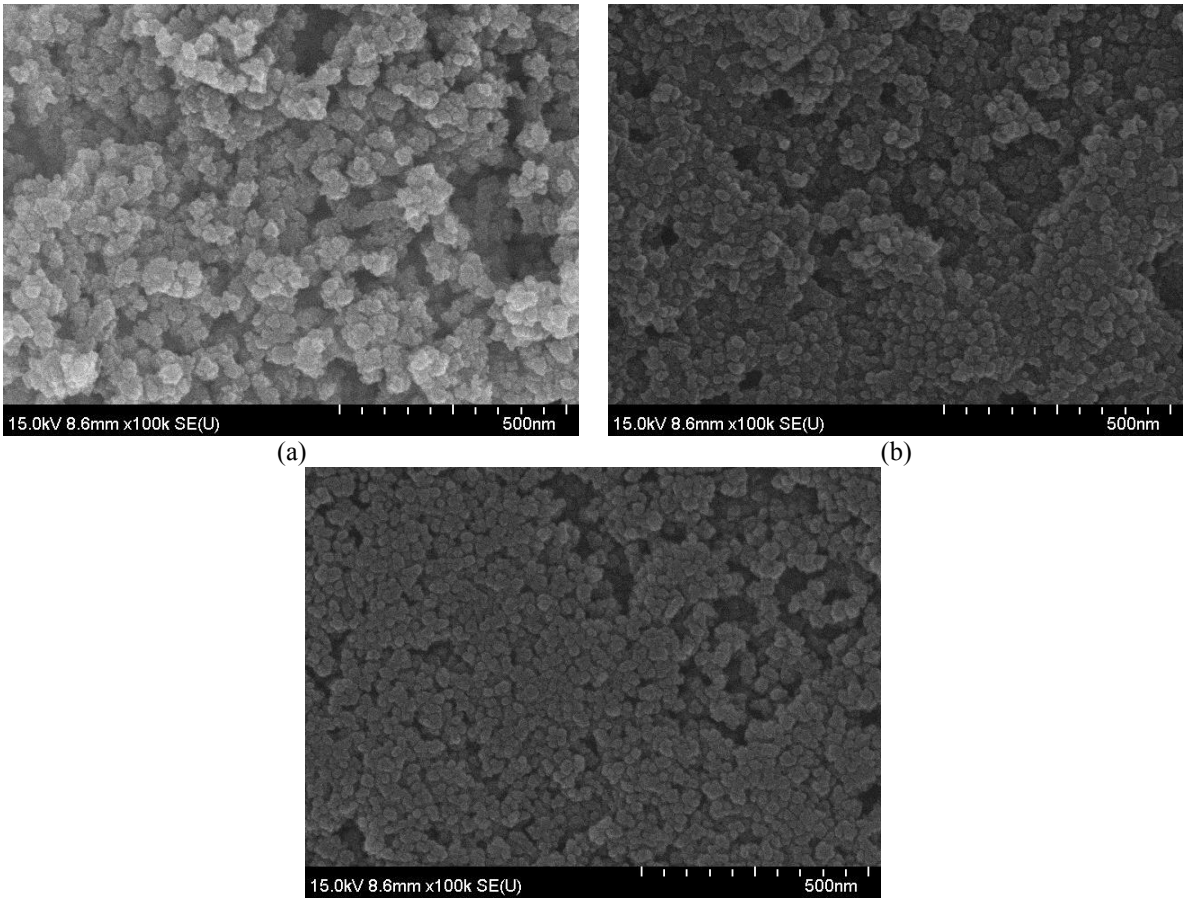

Fig. 7. FESEM image of the thin film; a) UndopedTiO_2 Thin film; b) 0.004 M Pr doped TiO_2 thin film; c) 0.008 M Pr doped TiO_2 thin film.

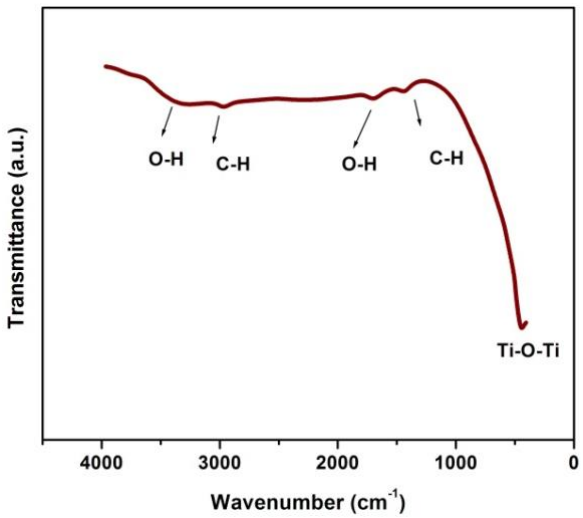

Fig. 8. FTIR spectra for high Pr-doped TiO_2 thin film

Fig. 9(C) shows the gas response and recovery behavior of 0.008 M pr doping, indicating resistance from 2.5×10^6 Ω (air) to 1.07×10^6 Ω (gas) and response times of 98 s, recovery time 33 s, respectively. However, deep quenching of defects accomplished by high doping exerts intense negative manipulation on gas on the surface density, which may lead to pining of the surface Fermi level and decrease the sensor response [30]. Fig. 9(D) shows the sensitivity of the pure and Pr-doped TiO_2 sensor to 200 ppm of ethanol. The low-doped Pr has a much enhanced sensitivity to ethanol at 200°C, higher than that of the pure TiO_2 sensor. The conversion to O^{2-} or O^- at significant temperatures is helpful in the gas sensing mechanism, as only a monolayer of oxygen ions are present with these strongly chemisorbed species [31].

4. CONCLUSIONS

This work synthesized the structural, morphological, optical, and sensor properties of a Pr-doped TiO_2 thin film prepared by nebulizer spray pyrolysis deposition technique and also studied the gas sensor properties by calculating the sensitivity, response, and recovery time.

[DOI: 10.22068/ijmse.2892]

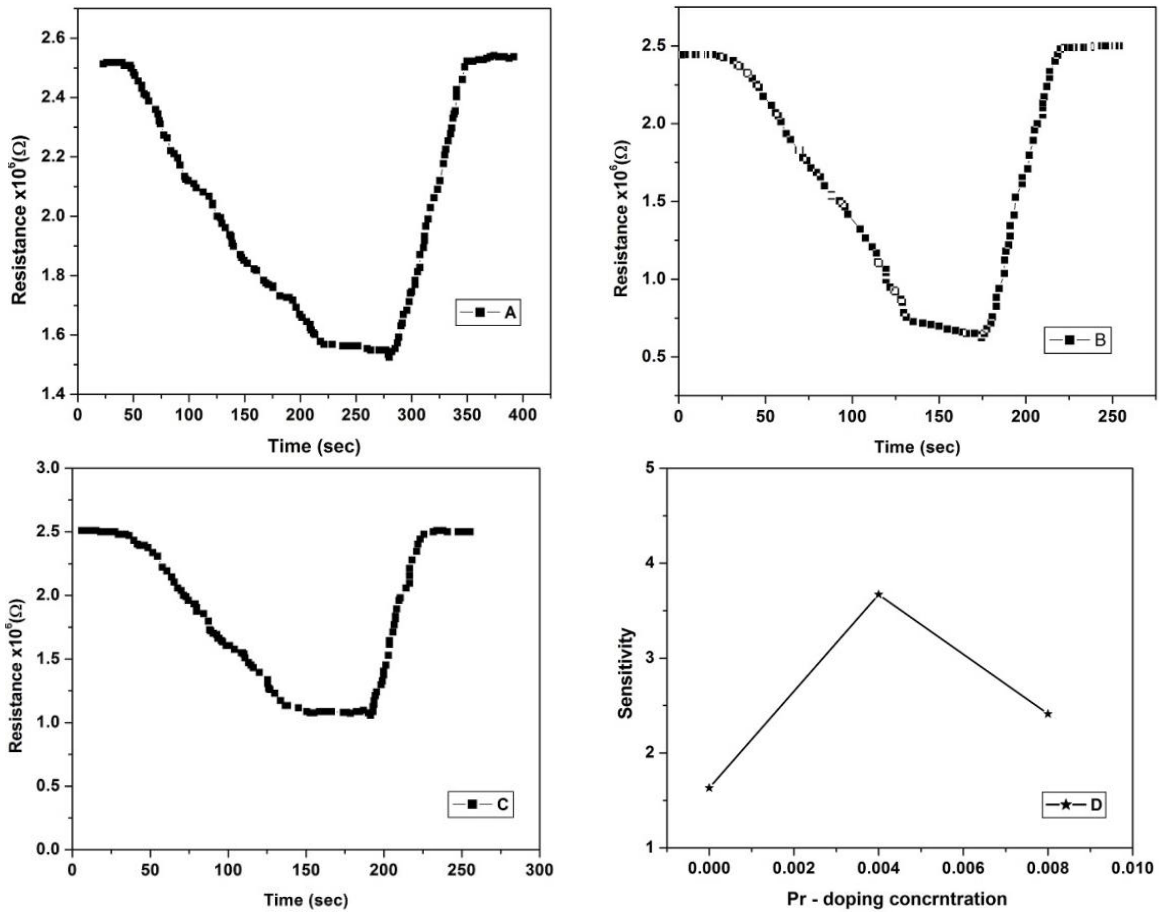

Fig. 9. Gas sensing curve (A) Undoped TiO_2 Thin Film (B) 0.004 M Pr Doped TiO_2 Thin Film (C) 0.008 M Pr Doped TiO_2 Thin Film (D) Sensitivity variation with doping

From X-ray diffraction analysis, Pr-doped TiO_2 thin films are polycrystalline, corresponding to the TiO_2anatase phase. The optical properties of TiO_2 showed that it had optical transparency in the visible region and it was observed that the optical band gap decreased when the doping ratio of TiO_2 was low, then increased a band gap value significantly at high doped TiO_2 thin film. The thin film's optical properties, such as its extinction coefficient and refractive index, were also discussed. The FTIR analysis shows the O-H hydroxyl groups and C-H bonds, which are characteristic of the TiO_2 anatase. The surface morphology of Pr-doped TiO_2 thin film is porous with agglomerated cluster nanocrystalline formation. Ethanol sensing tests indicate that working temperatures of 200°C cause more significant changes in the electrical resistance of Pr-doped TiO_2 gas sensors than the pure TiO_2 thin film.

REFERENCES

[1]. Uchida, S. Chiba, R. Tomiha, M. Masaki, N. Shirai, M. "Application of Titania Nanotubes to a Dye-sensitized Solar Cell." Electrochemistry., 2002, 70, 418-420.

[2]. Ravirajan, P. Haque, S.A. Durrant, J.R. Bradley D. D. C.and Nelson, J. "The Effect of Polymer Optoelectronic Properties on the Performance of Multilayer Hybrid Polymer/TiO_2 Solar Cells."Adv. Funct. Mater. 2005, 15, 609-618.

[3]. Kim, I. Choi, W. Y. "Hybrid gas sensor having TiO_2 nanotube arrays and SnO_2 nanoparticles." International Journal of Nanotechnology., 2017, 14, 155-165.

[4]. Kim, W.T. Kim, I.H. Choi, W.Y. (2015). "Fabrication of TiO_2 nanotube arrays and their application to a gas sensor." Journal of nanoscience and nanotechnology., 2015, 15, 8161-8165.

[5]. Kim, I. Choi, W.Y. "Hybrid gas sensor having TiO_2 nanotube arrays and SnO_2 nanoparticles." Int. J. Nanotechnol.,2017,

[DOI: 10.22068/ijmse.2892]

14, 155 - 165
[6]. Taurino, AM. Capone, S.Siciliano, P. Toccoli, T. Boschetti, A. Guerini, L. Iannotta, S. "Nanostructured TiO_2 thin films prepared by supersonic beams and their application in a sensor array for the discrimination of VOC." Sens. Actuators., 2003, 92, 292–302.
[7]. Kusior, A. Radecka, M. Zakrzewska, K. Reszka, A. Kowalski, BJ."Sensitization of TiO_2/SnO_2 nanocomposites for gas detection." J. Sens. Actuators B., 2013, 189, 251–259.
[8]. Gönüllü, Y. Haidry, A A .Saruhan, B. "Nanotubular Cr-doped TiO_2 for use as high-temperature NO_2 gas sensor." Sens. Actuators B., 2015, 217, 78–87.
[9]. Karunagaran, B. Uthirakumar, P. Chung, SJ. Velumani,S. Suh, EK. "TiO_2 thin film gas sensor for monitoring ammonia," Mater. Charact., 2007, 58, 680–684.
[10]. Ma, S. Jia, J. Tian, Y. Cao, L. Shi, S. Li, X. Wang, X. "Improved H_2S sensing properties of Ag/TiO_2 nanofibers." Ceram. Int., 2016, 42, 2041–2044.
[11]. Okuya, M. Prokudina, N. A. Mushika K. Kaneko, S. "TiO_2 thin films synthesized by the spray pyrolysis deposition (SPD) technique." Journal of the European Ceramic Society., 1999, 19, 903-906.
[12]. Abou-Helal, M.O. Seeber, W.T. "Preparation of TiO_2 Thin Films by Spray Pyrolysis to be Used as a Photocatalyst." Applied Surface Science., 2002, 195, 53-62.
[13]. Conde-Gallardo, A. Guerrero, M. Castillo, N. Soto, A.B. Fragso, R. Cabanas-Moreno, J. G. "TiO_2 anatase thin films deposited by spray pyrolysis of an aerosol of titanium diisopropoxide." Thin Solid Films., 2005, 473, 68-73.
[14]. Castaneda, L. Alonso, J. C. Ortiz, A. Andrade, E. Saniger, J. M. Banuelos ,J. G. "Spray pyrolysis deposition and characterization of titanium oxide thin films." Chem. Phy., 2002, 77, 938-944.
[15]. Takeda, S. Suzuki, S. Odaka, H. Hosono, H. "Photocatalytic TiO_2 thin film deposited onto glass by DC magnetron sputtering." Thin Solid Films., 2001, 392,338-344.
[16]. Leostean, C. Stefan, M. Pana, O. Cadis, A.I. Suciu, R.C. Silipas, T.D. Gautron, E. "Properties of Eu doped TiO_2 nanoparticles prepared by using organic additives." J. Alloys Compounds., 2013, 575, 29-39.
[17]. AlfaroCruz, M.R. Sanchez-Martinez, D. Torres-Martínez, L.M. "Optical properties of TiO_2 thin films deposited by DC sputtering and their photocatalytic performance in photoinduced process." International Journal of Hydrogen Energy, 2019, 44, 20017-20028.
[18]. Maniv, S. Zangvil, A. "Controlled Texture of Reactively rf-Sputtered ZnO Thin Films." J. Appl. Phys., 1978, 49, 2787–2792.
[19]. Swanepoel,R. (1984). "Determination of surface roughness and optical constants of inhomogeneous amorphous silicon films." J. Phys. E., 1984, 17, 896-903
[20]. Hasan, M.M. Hasseeb, A.S.M.A. Saidur, R. Masjuki, H.H. "Effect of annealing treatment on optical properties of anatase TiO2 thin films." International Journal of Chemical and Bimolecular Engineering., 2008, 1, 93-97.
[21]. Islam, M.R. Podder, J. "Optical properties of ZnO nanofibers thin films grownby spray pyrolysis of zinc acetate precursor." J. Cryst. Res. Technol., 2009, 44, 286–292.
[22]. Karakaya, S. Ozbas, O. "Preparation and Characterization of Highly Conducting and Transparent Conducting ZnO Thin Films by Ultrasonic Spray Pyrolysis." Can. J. Basic Appl. Sci., 2015, 3, 53–58.
[23]. Arunachalam, A. Dhanapandian, S. Manoharan, C. Sivakumar, G. "Physical properties of Zn doped TiO_2 thin films with spray pyrolysis technique and itseffects in antibacterial activity." Spectrochim. Acta. A., 2015, 138, 105–112.
[24]. Chen, J.L. Chen, D. He, J.J. Zhang , S.Y. Chen, Z.H. "The microstructure, optical, andelectrical properties of sol–gel-derived Sc-doped and Al–Sc co-doped ZnO thin films."Appl. Surf. Sci., 2009, 255, 9413-9419.
[25]. He, H.Y. "Optical and Electrical Properties of pure and Y-doped n-SnSe films deposited bychemical bath deposition." JOM., 2015, 67, 2071- 2078.
[26]. Pathan, HM. Desai, JD. Lokhande, CD. "Modified chemical deposition and physicochemical properties of copper

[DOI: 10.22068/ijmse.2892]

sulphide (Cu_2S) thin films."Appl Surf Sci., 2002, 202, 47- 56.
[27]. Swanepoel, R. "Determination of the thickness and optical constants of amorphous silicon." J. Phys. E., 1983, 16, 1214-1222.
[28]. Cosandey, F. Skandan, G. Singhal, A. "Materials and processing issues in nanostructured semiconductor gas sensors." JOM-e., 2000, 52, 1–6.
[29]. Barsan, N. Weimar, U. "Conduction model of metal oxide gas sensor." Journal of Electroceramics., 2001, 7, 143-67.
[30]. Brynzari, V. Korotchenkov G. Dmitriew, S. "Theoretical study of semiconductor thin films gas sensor: Attempt to consistent approach." J. Electron. Technology., 2000, 33, 225-235.
[31]. Korotcenkov, G. Brinzari, V. Pronin, I.A. Ham, M.H. Cho, B.K. "Metal Oxides for Application in Conductometric Gas Sensors: How to Choose?" Solid State Phenom., 2017, 266, 187–195.

[DOI: 10.22068/ijmse.2892]